Virtual-crystal approximation and alloy broadening of intersubband transitions in *p*-type SiGe superlattices

Z. Ikonić,* R. W. Kelsall, and P. Harrison
Institute of Microwaves and Photonics, School of Electronic and Electrical Engineering, University of Leeds, Leeds LS2 9JT, United Kingdom

(Received 24 January 2001; revised manuscript received 10 May 2001; published 10 September 2001)

The predictions of quantized state energies as calculated by the empirical pseudopotential method (EPM) and by the 6×6 $\mathbf{k}\cdot\mathbf{p}$ model, both within the virtual-crystal approximation (VCA), are compared for the case of SiGe based quantum wells grown in the [001] direction. Furthermore, the accuracy of the VCA is tested by performing the EPM calculation with enlarged supercells comprising a number of minimal-volume supercells with a number of different configurations of pure Si or Ge atoms over the lattice sites. The accuracy of the VCA is found to be excellent (with errors less than 1 meV), and the agreement between the EPM and $\mathbf{k}\cdot\mathbf{p}$ is very good for energies up to a few hundred meV away from the valence band top. Finally, the influence of alloy disorder on the transition matrix elements, and the broadening of intersubband transitions due to fluctuations of the alloy composition and atomic configuration, are discussed.

DOI: 10.1103/PhysRevB.64.125308 PACS number(s): 73.21.−b

I. INTRODUCTION

There has recently been an increased interest in intersubband transitions in *p*-type strained-layer SiGe based quantum wells, due to their possible use in intersubband quantum cascade lasers operating in the mid- to far-infrared wavelength range.[1] This follows a substantial body of work on infrared photodetectors using SiGe, e.g., Refs. 2–5, or III-V compounds, e.g., Refs. 5 and 6, which was largely related to the fact that hole intersubband transitions are optically active for both the perpendicular and the in-plane polarization of light. The approach commonly used to find the subband structure in the valence band (v.b.) is the 6×6 or, for intermediate or narrow gap semiconductors, the 8×8 $\mathbf{k}\cdot\mathbf{p}$ model. A recent study of the accuracy of the $\mathbf{k}\cdot\mathbf{p}$ model, as compared to the results of the more sophisticated empirical pseudopotential method (EPM),[7] has indicated that its accuracy in *p*-type AlGaAs based quantum wells is good for energies not far (a few hundred meV) from the v.b. top. In this paper we assess the accuracy of the 6×6 $\mathbf{k}\cdot\mathbf{p}$ model compared with the EPM method, where both are employed within the virtual-crystal approximation (VCA). We also investigate the accuracy of the VCA itself in SiGe based structures, which are necessarily strained, in contrast to those based on AlGaAs. This issue may be important, particularly given that SiGe structures have been considered for relatively short wavelength infrared intersubband lasers ($\lambda\sim2.2$ μm, i.e., with $\geqslant0.5$ eV transition energy[8]), where simplified methods of band structure calculation usually cease to be reliable. Furthermore, we discuss additional mechanisms of transition broadening in these structures, caused by fluctuations of the alloy composition about the nominal average, and fluctuations of the Si and Ge atomic configuration (which can only be modeled in calculations beyond the VCA). The issue of line broadening may also be important for the operation of SiGe based quantum cascade lasers, because it influences the value of achievable gain.

II. CALCULATION DETAILS

In present-day applications the SiGe structures almost always include at least one SiGe alloy layer, rather than only pure Si and pure Ge layers. In the VCA the atoms at lattice sites in alloy layers are all assumed identical, and their form functions are taken as the weighted average of the Si and Ge form functions. Within the VCA approach the minimal supercell suffices for any calculation of interest. If the VCA is not used, then either a pure Si or a pure Ge atom must be specified at every site. In this approach there are clearly a number of different atomic arrangements over the available lattice sites (configurations) in the alloy layer, even when using the minimal unit cell. States obtained for such structures will normally show a spread of values. However, in order to decrease the influence of the rather short-scale in-plane periodicity introduced by using the minimal unit cell, larger unit cells may also be set up by stacking a number of minimal cells side-by-side. In this set of calculations we have used supercells comprising up to 8 minimal supercells. The well layer in the supercells was taken to be between 4 and 14 monolayers wide (where one monolayer equals half a lattice constant), and in the majority of cases the alloy was $Si_{0.5}Ge_{0.5}$, while the barriers were always 4 monolayers of pure Si. It was found that increasing the barrier width only increased the computation time, without providing any new information. Since the layers, especially the barriers, are rather thin (this was dictated by the available computer time and memory), these structures should be classified as superlattices, rather than isolated quantum wells. However, the results are also applicable to quantum wells with reasonable accuracy, since it is the well (alloy) layer which is mostly responsible for the effects considered here.

By comparing the results of the VCA EPM calculations with those obtained from the $\mathbf{k}\cdot\mathbf{p}$ model the reliability of the latter can be deduced, and also the amount of broadening arising from the fluctuations of the alloy composition about the nominal average. Only from the non-VCA EPM calculations can one find the accuracy of the VCA itself, and also

the amount of state broadening that arises due to fluctuations of atomic configurations. It was assumed that no clustering effects occured in the alloy layers. The electronic structure of random alloys has been the subject of a number of papers in the past decade. Some alloy properties may be calculated by using ''special quasirandom structures,''[9] i.e., by finding the electronic structure of only a small number of relatively small-sized supercells designed to mimic, as far as possible, the atomic type correlations that exist in a random alloy. This approach would suffice for testing the accuracy of VCA, but for the purpose of estimating the alloy broadening and its scaling with the supercell size, we adopt the ''direct sampling method,''[9] in which the electronic structure for a large number of supercells with different atomic configurations is calculated. The configuration was randomly reshuffled in each run, and a sufficiently large number of calculations was made to obtain statistically converged results. Both mechanisms of broadening can be classified as ''band-structure-induced;'' i.e., they appear as broadening relative to a simpler description of the electronic structure (e.g., the $\mathbf{k}\cdot\mathbf{p}$ employed within the VCA), but should be distinguished from the scattering (dephasing and lifetime) induced broadening that also arises due to these and other effects (phonons, carrier-carrier scattering, etc.).

The EPM was implemented as a supercell calculation, with spin-orbit coupling included. The atomic potentials of Si and Ge atoms are described by appropriate form functions $V(q)$. The layers in SiGe superlattices are strained and, consistent with the model of homogeneous strain in individual layers, as is also used in the $\mathbf{k}\cdot\mathbf{p}$ model, the atomic coordinates in the supercell are taken as the strain-scaled ideal ones. The size of the conventional, minimum-volume (''minimal'') supercell in the growth direction is equal to the superlattice period, and its cross section in the growth plane equals $a_s^2/4$, where a_s is the in-plane lattice constant set by the substrate (this value applies to the case of [001] growth, considered here). The cutoff energy was set to 4.5 Ry in order to save the computational time and memory (this is very important in large supercell calculations).

The 6×6 $\mathbf{k}\cdot\mathbf{p}$ model was implemented by using a Fourier expansion of the wave functions[10] and the Burt-Foreman boundary conditions.[11] The structure is thus implicitly taken to be periodic (i.e., a superlattice), as in the EPM calculation. In alloy layers the deformation potentials are taken as weighted averages of those for Si and Ge. As for the values of Luttinger γ parameters in alloy layers, it has been found that, among various possibilities, the best scheme involves finding the hole effective masses in Si and Ge, making their linear interpolation for the alloy, and then transforming back into γ parameters.[12,13] In normal $\mathbf{k}\cdot\mathbf{p}$ calculations one uses the material parameters extracted from experiments. Such parameters feature implicitly in the EPM, but their values do not quite agree with the experimental values. For the purpose of comparison it is essential that the two calculations do actually use, explicitly or implicitly, the same set of parameters (the γ parameters, deformation potentials, and the average v.b. offset ΔE_v), and it is preferable that these are reasonably close to the accepted experimental values. The γ parameters implicit to the EPM are extracted from the dispersion of the HH, LH, and SO bulk bands along the [001] or [111] directions. However, the problem is overdetermined (there are more equations than γ parameters).[7] The precision of the results is a few percent, which should be borne in mind when comparing the EPM and $\mathbf{k}\cdot\mathbf{p}$ results. The deformation potential b is found from the HH-LH splitting after applying strain (i.e., alloy substrate) to Si or Ge, while a_v and ΔE_v are found from the differences of the v.b. tops in the unstrained and strained cases (the $Ge_{0.5}Si_{0.5}$ substrate was used). Extraction of these parameters also suffers from overdeterminancy. The Si and Ge form functions from Ref. 14 are found to be better in this respect than any other sets we have tested. While originally employed with a rather large cutoff energy of 8.0 Ry, they work very well even with a cutoff of 4.5 Ry, with only the valence band edge discontinuity being significantly affected. The bulk parameters implicit to the EPM are $\gamma_1=4.34$ (9.12), $\gamma_2=0.37$ (2.76), $\gamma_3=1.30$ (3.78), b [eV] $=-2.39$ (-2.75), and a_v [eV] $=2.46$ (1.24) for Si (Ge), showing good overall agreement with values often used in regular $\mathbf{k}\cdot\mathbf{p}$ calculations, e.g., Ref. 15: $\gamma_1=4.22$ (13.4), $\gamma_2=0.39$ (4.25), $\gamma_3=1.44$ (5.69), b [eV] $=-2.10$ (-2.86), and a_v [eV] $=2.46$ (1.24) for Si (Ge). The value of ΔE_v implicit in the EPM calculation is 0.438 eV, somewhat lower than the value proposed in Ref. 16 (0.58 eV), but still good enough for the present purpose (in fact, many calculations use an apparently better estimate, 0.54 eV, even closer to the value implicit to the EPM).

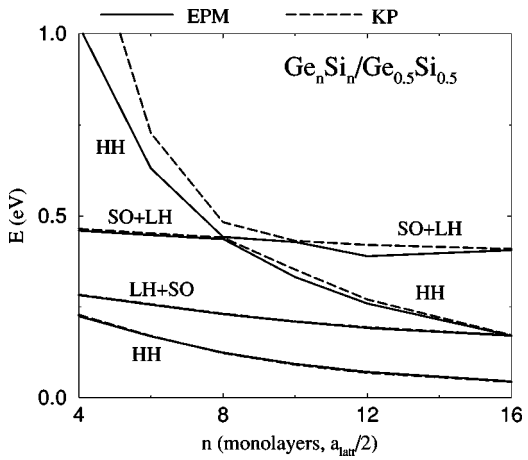

FIG. 1. Subband energies at $k_{||}=0$, calculated by the VCA EPM (solid lines) and the $\mathbf{k}\cdot\mathbf{p}$ method (dashed lines) for Ge_nSi_n superlattices on a $Ge_{0.5}Si_{0.5}$ virtual substrate.

III. NUMERICAL RESULTS AND DISCUSSION

A comparison of the results from the $\mathbf{k}\cdot\mathbf{p}$ model and the VCA EPM is shown in Figs. 1 and 2. In Fig. 1 the subband energies (measured downwards from the HH v.b. top in the well) are given for Ge_nSi_n superlattices ($n=4-16$) on a $Ge_{0.5}Si_{0.5}$ virtual substrate. Clearly, the degree of agreement is quite good for energies below $\sim$400 meV, even for the shortest-period structure (Ge_4Si_4) but decreases considerably at higher energies. Similar results are obtained in other structures, with alloy wells and/or barriers. The in-plane dispersion of subbands in the Ge_4Si_4 superlattice is given in Fig. 2.

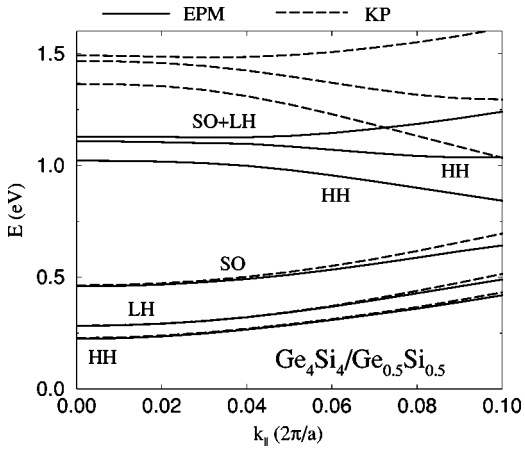

FIG. 2. The in-plane dispersion of the subbands (with $k_{||}$ along the $\langle 10 \rangle$ direction) calculated by the VCA EPM (solid) and the $\mathbf{k}\cdot\mathbf{p}$ method (dashed lines), for a Ge_4Si_4 superlattice on a $Ge_{0.5}Si_{0.5}$ virtual substrate.

At low energies the agreement is very good, slowly degrading as the in-plane wave vector $k_{||}$ increases. Actually, even for high-energy states the *dispersions* agree reasonably well; the discrepancy is primarily due to the quantized part of energy. That there is some discrepancy between the $\mathbf{k}\cdot\mathbf{p}$ and EPM, and that it increases as either the $k_{||}$ or the quantized state energy (i.e., the equivalent perpendicular wave vector in the well, k_z) increases, is in accordance with physical expectations. This is mostly due to the fact that the overlap of the off-zone-center bulk states and states at zone center decreases as $k_{||}$ or k_z increase (an inadequacy of the $\mathbf{k}\cdot\mathbf{p}$ model even for bulk material[7]). However, the discrepancy is sufficiently small not to warrant any concern over use of the $\mathbf{k}\cdot\mathbf{p}$ method. It should be noted that an apparently larger discrepancy may occur in very wide wells, having a very dense spectrum; this is due to a large interaction of states which amplifies the discrepancy between the $\mathbf{k}\cdot\mathbf{p}$ and EPM results. This does not mean that the $\mathbf{k}\cdot\mathbf{p}$ method is unreliable, however. Similar discrepancies would occur when using different sets of material parameters that have appeared in the literature. It is unlikely that any method could provide good agreement with experiment in such cases.

Concerning the accuracy of the VCA in SiGe system, we have found that it is very good indeed. The configurational averages of non-VCA state energies agree with the VCA predictions to better than 1 meV. Interestingly, this conclusion cannot be reached by considering only the averages for minimal supercells, which give a discrepancy of a few meV, but supercells of twice the minimal supercell volume are sufficient to confirm the excellent accuracy of the VCA.

We have also analyzed the spread of the energy values obtained for different atomic configurations. The mean square deviation of the energies may be interpreted as a broadening of states, and will thus be denoted as Γ. As the number of configurations increased it was found that Γ stabilized (i.e., became statistically significant) to a value specific to the supercell considered and to the type of quantized state. For a given superlattice period Γ steadily decreases as the number of minimal supercells, N_{cell}, in the supercell (i.e., the "averaging area") increases, as illustrated in Fig. 3. Interestingly, the distribution of state energies is not symmetric—it is steeper on the high energy side—but the mean value is in excellent agreement with the VCA result. As N_{cell} increases the maximal excursion of energies remains constant, for obvious reasons—the increased volume supercells have all the configurations present in smaller supercells repeated, along with many others—and may be at least 50 meV for long-period supercells. However, the configurations which do lead to such deviant state energies become very rare for larger N_{cell}, and it is the mean square deviation which matters for physical properties. On the other hand, Γ increases with the well width, being approximately 4.4 (1.4) meV for the lowest HH (LH) state in a 4 monolayer well, but converging for widths larger than about 12 monolayers to approximately 12.5 (7.0) meV for the lowest HH (LH) states therein. The dependence of Γ on the well width is in accordance with the random potential theory (e.g., Ref. 17) where the random part of the potential in this case is the deviation of the microscopic, atom-type-dependent potential from the periodic VCA potential. The shift ΔE of energy states in the presence of a random potential V_{rand} may be described by second order perturbation theory (the first order does not contribute, due to symmetry[17]), i.e., $\Delta E_i = \Sigma_{j\neq i}\langle\psi_j|V_{\text{rand}}|\psi_i\rangle/(E_i - E_j)$. The shift of a state is thus proportional to the square of its probability density taken in the well region (where the random potential is present), and indeed we do find such a trend as the number of monolayers increases. The dependence of Γ on N_{cell} is reasonably well fitted to an exponential relationship of the form $\Gamma = \Gamma_0 \exp(-\alpha N_{\text{cell}})$, as suggested in Ref. 7. For narrow wells the value of Γ_0 is about equal to Γ and the exponent α is small (~ 0.2), but for the (practically more important) wider wells, Γ_0 stabilizes at ~ 20 meV (~ 10 meV) for the HH (LH) state, and the exponent to $\alpha \sim 0.5$. A slightly larger value of Γ applies to the second HH bound state which appears in wider wells.

The influence of alloy disorder on interband transitions in direct gap semiconductors has been extensively studied.[18,19] This tends to reduce the optical transition matrix elements. To the best of our knowledge, no such study has been done for the case of intersubband transitions, within either the valence or conduction band, in quantum well heterostructures. We have therefore calculated the transition matrix elements for the range of atomic configurations in the supercells mentioned above. The configurational average of the momentum matrix element squared for the HH1-HH2 transition (allowed at $k_{||}=0$) was found to be consistently lower by $\approx 5-6\,\%$ from the VCA value, independent of the supercell size, indicating an intrinsic effect of alloy disorder (similar factors of matrix element reduction have been found for interband transitions in InGaAlAs alloys[18]). Inspection of the results for individual configurations shows that those which have larger transition energies generally have larger transition matrix elements [this is similar to the situation for interband transitions in GaInN (Ref. 19)], but there is only a correlation, rather than a strict correspondence of the two. The difference between VCA and non-VCA results, however, decreases with increasing $k_{||}$. As for the HH1-LH1 transi-

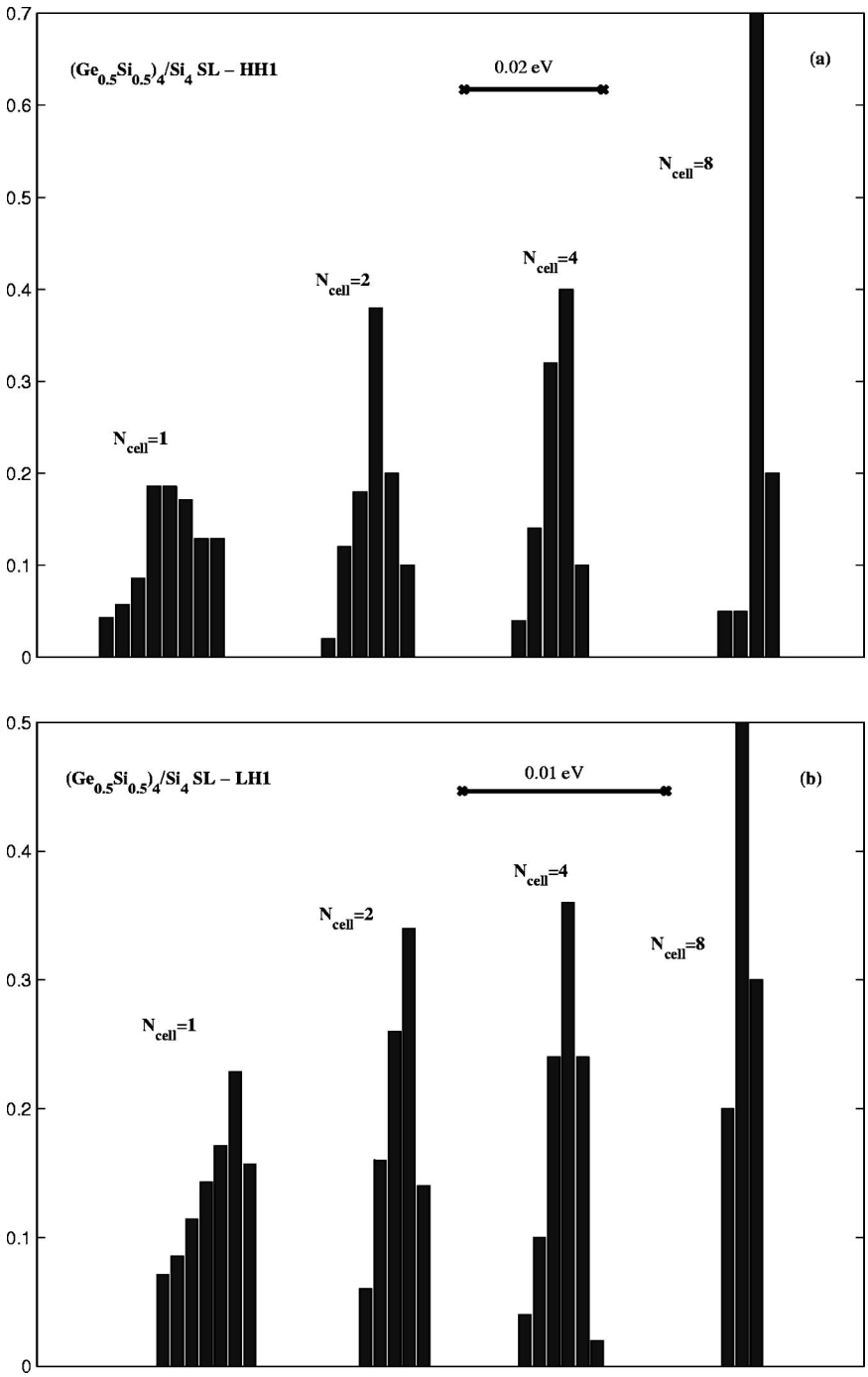

FIG. 3. The spread of zone-center energies for the HH1 (a) and LH1 (b) states in a $(Ge_{0.5}Si_{0.5})_4/Si_4$ superlattice on a $Ge_{0.25}Si_{0.25}$ virtual substrate, as it depends on the number N_{cell} of minimal supercells in the computational supercell, calculated with a number of random atomic configurations in the well layer.

tion, this is forbidden at $k_{||}=0$ in (nominally) symmetric structures. Beyond VCA, however, almost all the configurations have some asymmetry, so the HH1-LH1 transition is allowed even at $k_{||}=0$, but the matrix elements are very small. Calculations for nonzero $k_{||}$, where HH1-LH1 becomes fully allowed, do not reveal a statistically significant difference between the VCA and non-VCA results for this transition.

The finite Γ corresponding to individual states will translate into a broadening of the transition energies. Concerning the transitions between the lowest HH and LH states, we find that the shifts of the two states due to the random potential are rather highly correlated, and in fact the relation $\Gamma_{\mathrm{HH1\text{-}LH1}} \approx |\Gamma_{\mathrm{HH1}} - \Gamma_{\mathrm{LH1}}|$ applies to high accuracy. This is due to the fact that the wave functions of the two states are roughly similar. When both states are HH-like in character, we find that the shifts of HH1 and HH2 are only weakly correlated; i.e., $\Gamma^2_{\mathrm{HH1\text{-}HH2}} \approx \Gamma^2_{\mathrm{HH1}} + \Gamma^2_{\mathrm{HH2}}$ (the exact equality would apply to fully independent random variables), because their wave functions are now quite different, so broadening of HH1-HH2 transitions will be larger than that of HH1-LH1 transitions. All the above conclusions are valid at $k_{||}=0$, and apply to both states within the degenerate pairs (note that within the $\mathbf{k}\cdot\mathbf{p}$ method these would be the eigenvalues the two blocks of the Hamiltonian, and the EPM calculation confirms the degeneracy). For nonzero $k_{||}$, however, these de-

generate pairs become split (because the random potential is almost always asymmetric), and there is a mixing of HH and LH states. The resultant effect on the Γ's of individual states is that they slightly increase, but also become more correlated, so the transition linewidths remain almost the same as for $k_{||}=0$. Due to the correlation of the transition energy and matrix element, the linewidth will be modified by the spread of matrix elements, though not substantially in real situations, because, as shown below, this component of the linewidth is often of minor importance.

Yet another source of line broadening, which can be described within the VCA (or, indeed, the $\mathbf{k}\cdot\mathbf{p}$ method), are the fluctuations of the average alloy composition within a finite averaging area. For the alloy layer of nominal average composition x (when taken over an infinite area), the mean square deviation of the composition in a region containing N atoms is $\langle(\Delta x)^2\rangle = x(1-x)/N$ in case of lattice matched systems, and is somewhat reduced in the case of lattice mismatch.[20] The transition linewidth stemming from this effect may be found directly by performing a $\mathbf{k}\cdot\mathbf{p}$ calculation. However, an estimate may be obtained as follows. The deviation of the local composition average by Δx changes the strain conditions, separating the HH and LH band edges by $\Delta U = 2(1+2C_{12}/C_{11})(\Delta b - a_s \Delta a/a^2)\cdot\Delta x$, where $\Delta a = a_{\mathrm{Ge}} - a_{\mathrm{Si}}$ and $\Delta b = b_{\mathrm{Ge}} - b_{\mathrm{Si}}$ are the differences in the lattice constants or shear deformation potentials in Ge and Si, a is the lattice constant of the alloy, and C_{11} and C_{12} are the elastic constants (their ratio is assumed constant for simplicity). In addition, a change of composition influences the quantized part of the state energies via the Luttinger parameters, which may be estimated from the infinitely deep well formula as $\Delta E = (\hbar^2\pi^2/2m_0 d^2)(\Delta\gamma_1 \pm 2\Delta\gamma_2)$, where d is the well width. For wider wells (with 20 or more monolayers) this latter contribution is much less significant than the former in case of HH-LH transitions, but is the only one existing for the HH-HH transitions. In the language of perturbation theory, both comprise a first order perturbation. As an example of this type of broadening, for 10–20 monolayer wide $Si_{0.5}Ge_{0.5}$ quantum wells on $Si_{0.75}Ge_{0.25}$ substrate we find that $\Gamma[\mathrm{meV}] \approx 100\cdot N^{-1/2}$ for the HH-LH transition, and over four times smaller for the HH-HH transition. The number of atoms in a supercell comprising N_{cell} minimal supercells, for an n monolayers wide well, is $N = 2nN_{\mathrm{cell}}$.

Finally, to evaluate the contribution to intersubband linewidth due to alloy effects we have to assign some localization area to intersubband transitions. It is necessary for this localization area to be finite, otherwise there will be no broadening, because a particle would experience the existing potential as is—be it with some randomness or not. In the well studied cases of the broadening of excitonic or cyclotron resonance lines due to impurities, interface roughness, etc., there is a clearly defined localization area, and the same is true for transitions in confined structures (whether quantum confined or classically-sized pixels, as in Ref. 20). Such an area is less clearly defined for intersubband transitions, since there is apparently no in-plane localization of the carrier wave functions. Thus, we have taken the localization area to be a circle of one coherence length in diameter, where the coherence length is primarily determined by carrier-phonon and carrier-carrier scattering. In good-quality structures this is no less than ~ 100 Å, so with approximately $N_{\mathrm{cell}} = 10^3$ minimal cells in the localization area, and for a 20 monolayer (55 Å) well, the composition fluctuations will contribute approximately 0.5 meV to the linewidth, while the configurational contribution will be negligible. This broadening represents only a minor contribution to the total linewidth in quantum wells, which arises mostly due to scattering. However, both effects are expected to be much more pronounced in multidimensionally confined structures (quantum wires and dots), because of the greatly reduced number of atoms within the confinement volume. It may also be noted that whilst both these sources of line broadening will exist in the GaAs/AlGaAs system, they will be much weaker, since the quantum well layer therein is usually the unalloyed GaAs, so there is no alloy disorder in the region where most of the wave function is accumulated.

IV. CONCLUSION

By performing the VCA EPM, non-VCA EPM, and the 6×6 $\mathbf{k}\cdot\mathbf{p}$ calculations for strained SiGe structures we found that (i) the 6×6 $\mathbf{k}\cdot\mathbf{p}$ calculation is reasonably accurate in the energy range up to a few hundred meV away from the valence band top; (ii) the VCA is very accurate in the SiGe system; (iii) there is a broadening of transitions stemming from fluctuations of the average alloy composition (composition fluctuation broadening) and from fluctuations in the atomic type distribution over the lattice sites (configurational broadening); the former being much more important than the latter, but still constituting a relatively minor part of the total linewidth of intersubband transitions.

ACKNOWLEDGMENTS

This work is supported by DARPA/ USAF Contract No. F19628-99-C-0074. The authors thank W. Batty (Leeds) and R. A. Soref (Hanscom AFB) for useful discussions.

*Email address: z.ikonic@ee.leeds.ac.uk

[1] R. A. Soref, L. Friedman, and G. Sun, Superlattices Microstruct. **23**, 427 (1998).
[2] H. C. Liu, L. Li, J.-M. Baribeau, M. Buchanan, and J. G. Simmons, J. Appl. Phys. **71**, 2039 (1992).
[3] T. Fromherz, E. Koppensteiner, M. Helm, G. Bauer, J. F. Nützel, and G. Abstreiter, Phys. Rev. B **50**, 15073 (1994).
[4] P. Kruck, A. Weichselbaum, M. Helm, T. Fromherz, G. Bauer, J. F. Nützel, and G. Abstreiter, Superlattices Microstruct. **23**, 61 (1998).
[5] J. L. Pan, and C. G. Fonstad, Mater. Sci. Eng., R. **28**, 65 (2000).
[6] F. Szmulowicz, A. Shen, H. C. Liu, G. J. Brown, Z. R. Wasilewski, and M. Buchanan, Phys. Rev. B **61**, 13798 (2000).
[7] D. M. Wood and A. Zunger, Phys. Rev. B **53**, 7949 (1996).
[8] L. Friedman, R. A. Soref, G. Sun, and Y. Lu, IEEE J. Sel. Top. Quantum Electron. **4**, 1029 (1998).
[9] S.-H. Wei, L. G. Ferreira, J. E. Bernard, and A. Zunger, Phys. Rev. B **42**, 9622 (1990).

[10] D. Gershoni, C. H. Henry, and G. A. Barraf, IEEE J. Quantum Electron. **29**, 2433 (1993).
[11] B. A. Foreman, Phys. Rev. B **48**, 4964 (1993).
[12] C. M. de Sterke, Phys. Rev. B **36**, 6574 (1987).
[13] W. Batty, Ph.D. thesis, University of Surrey, Guildford, United Kingdom, 1990.
[14] P. Friedel, M. S. Hybertsen, and M. Schlüter, Phys. Rev. B **39**, 7974 (1989).
[15] A. Kahan, M. Chi, and L. Friedman, J. Appl. Phys. **75**, 8012 (1994).
[16] C. G. Van de Walle, and R. M. Martin, Phys. Rev. B **34**, 5621 (1986).
[17] V. M. Akulin, Phys. Rev. A **48**, 3532 (1993).
[18] J. C. Fan and Y. F. Chen, J. Appl. Phys. **80**, 1239 (1996).
[19] L. Bellaiche and A. Zunger, Phys. Rev. B **57**, 4425 (1998).
[20] M. W. Muller and A. Sher, Appl. Phys. Lett. **74**, 2343 (1999).